Chemically Cross-Linked Polycyclooctene: Synthesis, Characterization, and Shape Memory Behavior

Changdeng Liu, Seung B. Chun,† and Patrick T. Mather*

Polymer Program, Institute of Materials Science, University of Connecticut, Storrs, Connecticut 06268

Lei Zheng, Elisabeth H. Haley, and E. Bryan Coughlin*

Polymer Science and Engineering Department, University of Massachusetts, Amherst, Massachusetts 01003

Received July 17, 2002; Revised Manuscript Received September 20, 2002

ABSTRACT: A novel polymeric shape memory system of chemically cross-linked polycyclooctene (PCO) was developed and characterized. PCO was synthesized via ring-opening metathesis polymerization of cyclooctene using the dihydroimidazolylidene-modified Grubb's catalyst. After dicumyl peroxide was added to PCO, the mixture was compression-molded into a film and further cured through chemical cross-linking upon heating. The chemically cross-linked PCO samples were fully characterized using differential scanning calorimetry (DSC), dynamic mechanical analysis (DMA), and wide-angle X-ray scattering (WAXS) in order to gain insight into the rapid shape memory behavior. We observe that the transition temperature of PCO is tunable through the change of the trans/cis ratio of vinylene groups. A fast shape memory behavior was observed, where the primary stress-free shape was recovered within 1 s on immersion in hot water above the melting point of the crystalline PCO phase. In contrast with glassy shape memory polymers, chemically cross-linked PCO behaves as an *elastomer* capable of arbitrary shaping above the sharp melting temperature of the PCO crystalline phase and subsequent shape fixing during crystallization.

Introduction

Polymers intrinsically show shape memory effects, on the basis of rubber elasticity, but with varied characteristics of strain recovery rate, work capability during recovery, and retracted state stability. To the best of our knowledge, the first reported shape memory polymer (SMP) was a methacrylic acid ester by the Vernon-Benshoff Co. for use as a denture material.[1] However, the mechanism of strain recovery for such a material was immediately identified as far different from that of shape memory alloys (SMAs), based largely on nickel−titanium alloys. Indeed, a shape memory polymer is actually a super-elastic rubber: when the polymer is heated to a rubbery state, it can be deformed under resistance of ∼1 MPa modulus, and when the temperature is decreased below either a crystallization temperature or a glass transition temperature, the deformed shape is fixed by the lower temperature rigidity while, at the same time, the mechanical energy expended on the material during deformation is stored. Consequently, when the temperature is raised above the transition temperature (T_m or T_g), the polymer will recover to its original form as driven by the restoration of network chain conformational entropy. Figures of merit for SMPs will be closely linked to the network architecture and to the sharpness of the transition separating the rigid and rubber states. Compared with SMAs, SMPs have an advantage of high strain (to several hundred percent) because of the large rubbery compliance while the maximum strain of a SMA is less than 8%. Of additional benefit, the transition temperature can be tailored according to the application requirement, e.g., tuning the transition temperature as thermal sensors.[2] Accordingly, numerous polymers have been found to have particularly attractive shape memory effect, most notably the polyurethanes, polynorbornene, styrene−butadiene copolymers, and cross-linked polyethylene.[3]

Block copolymers of polystyrene (PS) and *trans*-polybutadiene (TPB) with minor PS content offer an alternative approach to shape memory with a distinct mechanism of strain fixation and recovery triggering.[4] While microphase-separated domains of the PS block are amorphous with $T_g \sim 93$ °C, the continuous TPB phase is semicrystalline with $T_g = -90$ °C and $T_m = 68$ °C. Because of the immiscibility between PS and TPB blocks below 120 °C, the copolymer forms microdomain structure with elastic rheological characteristics above the TPB melting temperature, with the PS phase serving the role of physical cross-linking. Thus, reversible deformations can be fixed by crystallizing the TPB phase below about $T = 40$ °C and recovered to the stress-free state (shape memory) upon heating above 80 °C to melt the TPB phase and free the elastically deformed material to recover strain.

Another semicrystalline shape memory polymer is *trans*-polyisoprene (TPI), a polymer with $T_m = 67$ °C and degree of crystallinity near 40%, which undergoes facile cross-linking with peroxides.[5] Below T_m the cross-linked TPI has a three-dimensional network, which is connected by both chemical cross-links and the crystalline regions. Above T_m the crystalline phase melts to become amorphous, with only the chemical cross-links remaining to maintain the primary shape with a rubber-like modulus. This primary shape is the form of the material at the time of chemical cross-linking by peroxide cure, normally occurring near $T = 145$ °C for 30

† Present address: Rogers Corporation, Rogers, CT.

* To whom correspondence should be addressed: e-mail patrick.mather@ uconn.edu, tel (860) 486-3542, fax (425) 732-7953; e-mail coughlin@mail.pse.umass.edu, tel (413) 577-1616, fax (413) 545-0082.

10.1021/ma021141j CCC: $22.00
Published on Web 11/27/2002

min followed by cooling to room temperature, during which time crystallization occurs. Like with PS−TPB block copolymers, elastic deformation of cross-linked TPI can be performed by heating the polymer above $T = 80$ °C, and this deformed secondary shape may be fixed by cooling-induced crystallization. The deformed shape returns to the primary form upon heating above 80 °C. More recently, copolymers of semicrystalline polycaprolactone (PCL) have also been selected for its attractive SMP characteristics.[6]

We have recently carried out experimental investigations on the preparation and shape memory characterization of chemically cross-linked polycyclooctene (PCO). The PCO was synthesized from *cis*-cyclooctene to have a high trans double bond content; this polymer was subsequently chemically cross-linked with variation in cross-link density to form a semicrystalline thermoset SMP. In this paper, we present results on the polymer synthesis and on thermal, mechanical, and microstructural properties, as they depend on the extent of cross-linking, and give additional attention to the excellent shape recovery characteristics of cross-linked PCO—especially the rapid rate of strain recovery.

Experimental Section

Materials. The ruthenium catalysts bis(tricyclohexylphosphine)benzylidene ruthenium(IV) dichloride (**1**, Grubb's catalyst) and tricyclohexylphosphine[1,3-bis(2,4,6-trimethylphenyl)-4,5-dihydroimidazol-2-ylidene] [benzylidene] ruthenium(IV) dichloride (**2**) were purchased from Strem Chemical. Other reagents were obtained from Aldrich and used as received unless otherwise indicated; c*is*-cyclooctene was vacuum-distilled from CaH_2 prior to use. Methylene chloride was passed through columns of basic activated alumina prior to use.

Synthesis and Molecular Characterization of PCO. To a solution of 5.1 mg (6.0 μmol) of the ruthenium catalyst **2** in 50 mL of CH_2Cl_2 was added 6.60 g (60 mmol) of *cis*-cyclooctene. The reaction mixture was stirred under air for 30 min at room temperature, during which time it gelled. The reaction was stopped by injection of 50 mL of CH_2Cl_2 containing a trace amount of ethyl vinyl ether. The polymer was precipitated using methanol, recovered by filtration, and dried overnight under vacuum at room temperature. The isolated yield was 5.0 g (75%). ^{13}C NMR spectra were recorded in chloroform-*d* on a Bruker DPX-300 FT NMR spectrometer operating at 75 MHz. Quantitative spectra were obtained using a standard inverse-gated proton decoupling pulse sequence and a relaxation delay of 2 s to obtain trans/cis ratios. Gel permeation chromatography was performed using a Polymer Lab LC1120 HPLC pump equipped with a Waters differential refractometer detector. The mobile phase was tetrahydrofuran (THF), and a flow rate of 1 mL/min was employed. Separations were performed using a set of 10^5, 10^4, and 10^3 Å Polymer Lab columns. Molecular weights were calibrated vs narrow molecular weight polystyrene standards.

PCO Peroxide Curing.[7,8] PCO and dicumyl peroxide were dissolved in $CHCl_3$ to form a clear solution. The solution was dried in a fume hood at room temperature for 12 h and vacuum-dried in an oven at 40 °C for 12 h. Dried PCO containing DCP was transferred to a mold of dimensions 1 × 3 × 0.05 cm. The mold was placed between two hot platens and compressed at 140 °C under a pressure of 1000 psi for 30 min to yield a sheet specimen. After curing, the specimen was cooled to room temperature in the mold.

Thermal Characterization. Thermal properties (melting and crystallization temperatures) of cured PCO were measured using a Perkin-Elmer differential scanning calorimeter (DSC-7) using a first heating rate of 10 °C/min from −50 to 100 °C, a first cooling rate of −10 °C/min from 100 to −50 °C, and a second heating rate of 10 °C/min from −50 to 100 °C.

Table 1. Molecular and Thermal Characteristics of PCO Polymers

sample code	catalyst	monomer: catalyst ratio[a]	reaction time (h)	M_w (kg/mol)	PDI	trans (%)	T_m[b] (°C)
PCO1	1	500	2	127	1.55	68	41
PCO2	1	1000	2	194	1.65	n.d.	30
PCO3	1	2000	2	246	1.73	n.d.	19
PCO4	1	1000	19	183	1.64	78	55
PCO5	2	10000	0.5	315	2.00	81	60

[a] Monomer concentration 1.2 M. [b] Data are gathered on the second melt scan with 10 °C/min cooling history.

X-ray Scattering Methods. Wide-angle X-ray scattering (WAXS) analysis was performed using a Bruker GADDS-4 instrument with a Cr source of radiation (λ = 2.291 Å), operating in transmission mode. The voltage and the current used were 40 kV and 40 mA, respectively, and the exposure time was 30 min. The scattering patterns were collected on a HiStar area detector with the distance of the sample to detector set to 6.0 cm. Intensity profiles (I vs 2θ) were determined from azimuthal averaging at each 2θ position of the isotropic patterns. The data were then analyzed with Peakfit software (SPSS Science) to find the peak positions and the relative intensity of each peak.

Dynamic Mechanical Analysis. A TA Instruments DMA 2980 was run in tensile mode at an oscillation frequency of 1 Hz, a static force of 10 mN, an oscillation amplitude of 5.0 μm (∼0.1% strain), and an automatic tension setting of 125%. Temperature ramps were conducted at 4 °C/min over the range $-100 < T < 100$ °C.

Shape Memory Effect. PCO samples of varying cross-linking degree were cut into rectangular strips with dimension of 0.5 × 2.0 × 30.0 mm and colored with red dye to yield optical contrast. The PCO strips were bent in semicircular shape with an inner diameter of 0.737 cm in a warm water bath at 70 °C (at which temperature the samples are transparent and flexible) and then transferred into an ice water bath to fix the secondary bent shape by crystallization. The bent PCO samples were promptly dipped into the warm water bath at 70 °C, while recording images of shape recovery using a video camera at a rate of 20 frames/s. The variations of radius of curvature of the bent samples were analyzed using nonlinear regression (Sigmplot).

Results and Discussion

Synthesis. Polycyclooctene (PCO) can be synthesized using either $RuCl_2(=CHPh)(PCy_3)_2$, **1** (Grubb's catalyst),[9] or the dihydroimidazolylidene-modified Grubb's catalyst, **2**, but with catalyst **2** having a much higher reactivity compared with catalyst **1**.[10] It is noteworthy that a unique feature of PCO as a shape memory material is the tunable transition temperature (T_m of PCO), where a temperature range from 19 to 61 °C is achievable following the dependence of the melting point of PCO on the trans content of double bonds along the polymer backbone.[11] Our synthetic approach has the ability to control the trans/cis ratio as well as molecular weight by changing conditions: reaction time, catalyst type, and catalyst concentration. Thus, Table 1 shows representative examples of PCO variations achieved in this manner. In general, higher catalyst concentrations result in higher trans concentration and lower molecular weights (samples 2 and 3 vs 1). Additionally, prolonged reaction times (sample 4 vs 2) or the use of highly reactive catalyst **2** (sample 5) yield higher melting temperature products, presumably as a consequence of more cross-metathesis occurring between polymer chains, resulting in the thermodynamically more favorable trans products. In the following study, sample 5 was

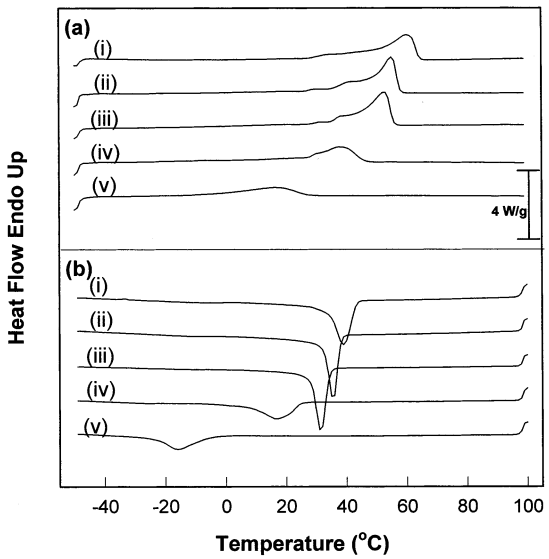

Figure 1. DSC traces of first heating (a) and cooling (b) for cured PCOs having varying amounts of peroxide. The ramping rates of 10 and −10 °C/min were used in heating and cooling cycles, respectively: (i) DCP 0%, (ii) DCP 1%, (iii) DCP 2.5%, (iv) DCP 5%, and (v) DCP 10%.

Table 2. Thermal Characteristics of Cured PCO

sample code	added peroxide/%	T_m/°C	T_c/°C	ΔH/J g^{-1}
PCO5−0	0	60.3	39.0	57.8
PCO5−1	1	55.2	35.5	62.8
PCO5−2.5	2.5	52.7	31.3	54.7
PCO5−5	5	38.2	16.8	35.1
PCO5−10	10	16.7	−16.0	22.9

chosen for in-depth characterization, based upon its desirable melt transition temperature and molecular weight.

Thermal Analysis. Figure 1 shows DSC traces of first heating (a) and cooling (b) for cured PCOs prepared using varying concentration (wt %) of peroxide: (i) DCP 0%, (ii) DCP 1%, (iii) DCP 2.5%, (iv) DCP 5%, and (v) DCP 10% to reveal its melting and crystallization behavior. The neat PCO was compression-molded in a hot press using the same conditions as for cross-linked PCO to provide an identical thermal history. During the first heating cycle (upper curve), neat PCO shows a melting temperature at 60.3 °C while any glass transition for neat PCO was not detected over the range −50 < T < 100 °C. According to Calderon and Morris,[11] the crystalline melting point for PCO depends linearly on the percentage of *trans*-vinylene content in the polymer; specifically, T_m = 60 °C was reported for 78% *trans*-vinylene content in PCO. For our neat PCO sample, the content of *trans*-vinylene is 80.6%, so that the measured melting transition of 60.3 °C is in good agreement with prior literature.[11] During the first cooling cycle (b(i)), neat PCO shows a crystallization exotherm at 39 °C. A second heating cycle shows the same result as the first heating cycle.

Cross-linking PCO with dicumyl peroxide has a dramatic impact on its crystallization and melting behavior. The melting point, T_m, the crystallization point, T_c, and the melting enthalpy (related to degree of crystallinity), ΔH, obtained from Figure 1 are summarized in Table 2. A significant effect of the degree of cross-linking is observed: both T_m and T_c of PCO decrease as the amount of DCP increases, the former by more than 40 °C for 10% DCP cross-linking. The melting enthalpy also decreases with increased cross-linking, indicating a decrease in degree of crystallinity. When the temperature is decreased below T_c, the constituent PCO chains begin to crystallize, the crystals growing to a certain final size and shape. In the case of neat PCO (without cross-linking points), we envision relatively low restriction for PCO crystal growth due to high polymer chain mobility. However, for the samples of increasing cross-link density, the polymer chains are constrained against diffusion and conformational rearrangement, thus increasingly restricting crystallization. As a result, higher peroxide loadings give rise to a reduced degree of crystallinity and concomitant reduction of crystal size, the latter inferred from the observed depression in melting temperature. It also can be seen from Table 2 that the melting temperature of cured PCO can be tailored by controlling the loading of peroxide before curing. Moreover, when the amount of peroxide exceeds 10%, the cured PCO shape memory behavior is lost as both T_m and T_c are below room temperature, and (as will be shown with DMA) the melting transition is broadened excessively.

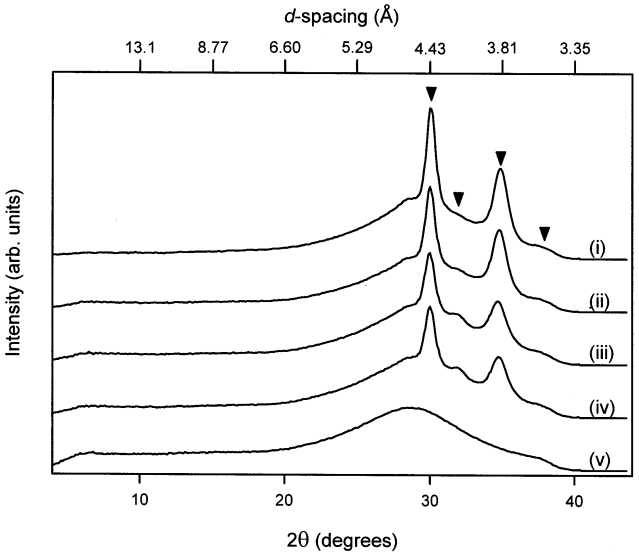

Figure 2. Intensity vs scattering angle in WAXS data: (i) DCP 0%, (ii) DCP 1%, (iii) DCP 2.5%, (iv) DCP 5%, and (v) DCP 10%.

Crystalline Microstructure. To investigate the underlying microstructure of PCO as affected by cross-linking, we have employed wide-angle X-ray scattering (WAXS), the results of which are shown in Figure 2. From the intensity profiles of all PCO samples except the PCO5−10, traces (i)−(iv), we found that the microstructure is characterized by the superposition of an amorphous halo and four crystalline diffraction rings of nearly constant *d*-spacing, but with intensity that decreases with increasing extent of cross-linking. Figure 2, trace (ii) for example, shows two strong scattering peaks at 2θ = 30.02° (4.42 Å) and 34.81°(3.83 Å) that correspond to the 010 and 100/110 reflections of the PCO triclinic crystal structure, respectively. Additionally, there are two weak peaks, 2θ = 31.94° (4.16 Å) and 2θ = 36.97° (3.61 Å) corresponding respectively to the 110 and 201 reflections of the PCO monoclinic crystal structure.[12,13] In the figure, the arrowheads are positioned at the scattering angles of these primary reflections.

Table 3. Summary of the WAXS Results

sample code	peak area (%) at 2θ =				deg of crystallinity	E' at 28 °C (MPa)
	30.02°	31.94°	34.81°	36.97°		
PCO5−0	11.25	0	12.44	1.84	25.5	173.4
PCO5−1	9.85	0	11.77	2.21	23.8	136.1
PCO5−2.5	7.78	0.39	7.85	2.03	18.1	128.1
PCO5−5	7.38	0.39	7.53	2.04	17.3	67.7
PCO5−10	0	0	0	2.64	2.6	8.4

We analyzed the WAXS patterns to deconvolute the constituent reflections using Peakfit software, and the data are summarized in Table 3, along with a summary of DMA results (vide infra). From the analysis we found that the degree of crystallinity of PCO is 25.5% at room temperature, which is close to the results from DSC (28.8%), employing the enthalpy data of a pure crystal (216 J/g) from Schneider and Muller.[14] Additionally, the degree of crystallinity shows a monotonic decrease with increasing cross-linking, the same trend observed with DSC and also explained by a constraining effect of cross-linking points that limit the growth of crystals. Indeed, sample PCO5−10 (10% DCP cross-linking) did not show significant crystallinity at room temperature; however, this does not mean that the sample cannot crystallize. From the DSC data (Figure 1) we can see that a crystalline phase of PCO5−10 melts over the range $-15 < T < 30$ °C, while we did the WAXS analysis at room temperature (28 °C). At this temperature the melting is nearly complete, yielding a measured degree of crystallinity of only 2.6%.

In analyzing the scattering patterns for the area % of each peak, we found that the effect of cross-linking confinement on the degree of crystallinity depends on the associated crystal structure. While the triclinic peaks at 30.02° and 34.8° 2θ decrease linearly with cross-linking, the monoclinic peaks at 31.9° and 36.97° 2θ seem almost unaffected by the cross-linking. It is thus apparent that the triclinic crystal structure is more sensitive to the constraining influence of cross-linking, while the monoclinic crystal structure is more robust, although still a minor component.[13,14] A similar structural transition with decreasing crystallinity on cross-linking has been reported for polyethylene,[15] suggesting that this is a general phenomenon in polyolefins.

Dynamic Mechanical Properties. Chemically cross-linking PCO also has a direct impact on the thermomechanical properties, e.g., modulus vs temperature, through the establishment of a permanent network and indirectly through the morphological transitions discussed above. Revealing such effects by the use of DMA, Figure 3 shows plots of the tensile storage modulus (E') vs temperature for cured PCOs prepared with varying amounts of DCP. All of the PCO samples are characterized by a solidlike storage modulus (about 1.7 GPa) for temperatures below $T = -70$ °C with this modulus value being invariant to the cross-linking density. For temperatures above $T = -70$ °C, the apparent onset of T_g in the PCO samples, E' begins to decrease gradually to a level that is dependent on cross-link density, but spanning 0.05−0.5 GPa. The decrease in modulus with cross-linking in this temperature region can be understood from the results of DSC and WAXS that showed cross-linking reduces the degree of crystallinity of PCO. We can now expect that the crystalline phase will function as both the fixing mechanism for shape memory and a means of controlling room temperature modulus over a full order of magnitude. For temperatures nearing $T = 62$ °C, close to the melting temperature measured by DSC, the storage modulus of neat PCO begins to decrease sharply to about 2 MPa at the completion of melting at 71 °C. As observed thermally with DSC, this transition temperature is observed mechanically to decrease with increasing degree of cross-linking. For temperatures greater than T_m, the modulus of neat PCO, trace (i), continues to decrease to a point where the material flows like a viscous liquid, not showing a persistent rubbery plateau (Figure 3). This feature hampers the applicability of neat PCO for use as a shape memory polymer due to an inability to be deformed as a rubber above T_m without rapid stress relaxation. On the other hand, cured PCO, which contains just 1% peroxide, represented by trace (ii), is expected to allow significant shape memory effects owing to its persistent rubbery plateau above 72 °C. As the amount of peroxide increases, the rubbery plateau modulus increases, allowing for enhanced mechanical energy storage, but the transition temperature and the steepness of the transition decrease. In the case of PCO with 10% DCP, PCO5−10, shown as trace (v) in Figure 3, we observe thermomechanical response that is inconducive to shape memory effects as the fixing (crystallization) temperature is lower than room temperature so that shape fixing would require subambient cooling, and the temporary shape would be expected to drift via partial melting. In addition, the melting transition is too broad for dramatic strain recovery to be expected.

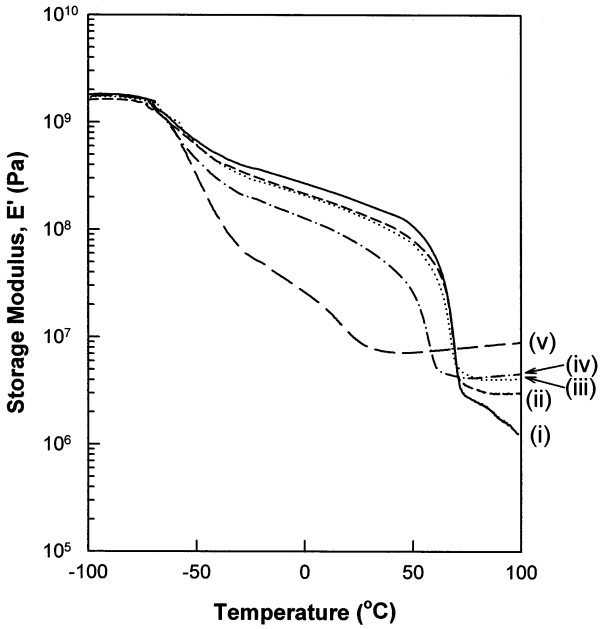

Figure 3. Tensile storage modulus (E') vs temperature for cured PCOs in a linear stress oscillation mode using 1 Hz of frequency and 4 °C/min of ramping rate: (i) DCP 0%, (ii) DCP 1%, (iii) DCP 2.5%, (iv) DCP 5%, and (v) DCP 10%.

From each of the curves in Figure 3, the onset (T_1) and the end (T_2) temperatures of the melting transition were determined, recognizing that shape memory behavior would benefit from a small difference in T_1 and T_2. Figure 4a depicts the influence of peroxide content on T_1 (○) and T_2 (△), noting that the onset of the temperature (T_1) corresponds closely to the melting point measured by DSC (Table 2). Both T_1 and T_2 decrease as amount of peroxide increases like T_m and T_c in Table 2, but more so for T_2. Figure 4b shows the difference in the onset and end transition temperatures, $\Delta T = T_2 - T_1$ (□), vs the amount of added peroxide; as

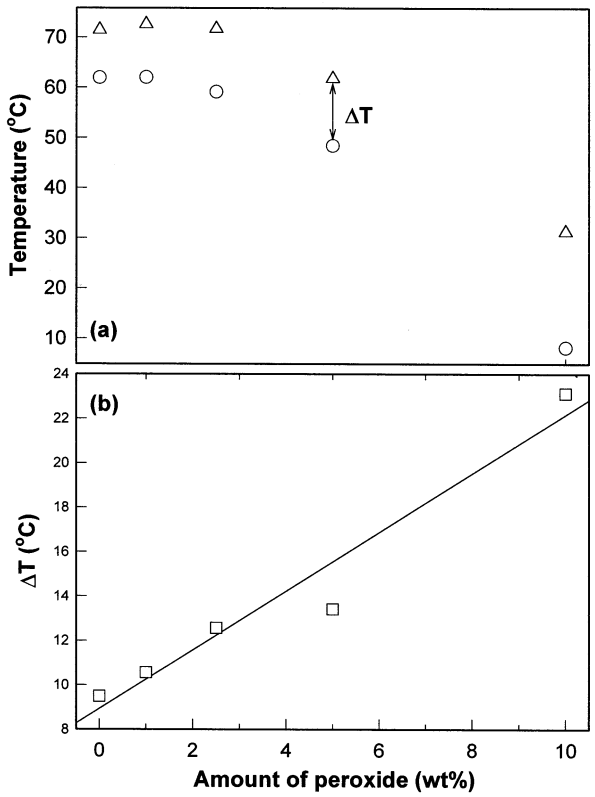

Figure 4. (a) Dependency of amount of added peroxide on T_1 (○) and T_2 (△) which are the onset and the end temperatures of transition, respectively, determined from curves in Figure 3. (b) ΔT (□) vs amount of added peroxide, where ΔT is the difference between T_1 and T_2.

the amount of peroxide increases, ΔT increases, indicating a loss in sharpness of the transition. We can also quantify the sharpness of this transition by measuring the maximum slopes of the E'−temperature trace in the melting region of Figure 3, and these results are shown in Figure 4. Clearly, a compromise between transition sharpness (high for neat PCO) and rubber elasticity (low for neat PCO) exists so as to influence the design of an optimal shape memory polymer.

We observe that the trend in thermomechanical behavior corresponds well with the WAXS data of Figure 2 and Table 3. In particular, we have found that the room temperature modulus decreases with increasing cross-linking, just as the degree of crystallinity decreases as observed with WAXS.

Shape Memory Effect. A typical example of the shape memory effect of PCO cured with 2.5 wt % DCP (PCO5−2.5) is shown in Figure 6. The primary, stress-free, shape of the sample under study was set at the cross-linking stage to be a linear rectangular bar (see picture at $t = 0.7$ s), while the secondary (temporary) shape was a semicircular film curved along the long axis and having an inner diameter of 0.737 cm (see picture at $t = 0$ s). Such a shape was achieved by heating the sample to a transparent state at $T = 70$ °C, deforming it to a semicircular shape using a pipet mandrel, and finally quenching the curved film in ice water, rendering the sample translucent white and leathery. We then examined shape recovery by rapidly submerging the curved sample into a water bath heated to $T = 70$ °C. As shown in Figure 6, the transition from the secondary shape to the primary shape is completed within $t = 0.7$ s. In contrast, an un-cross linked sample, PCO5−0, does

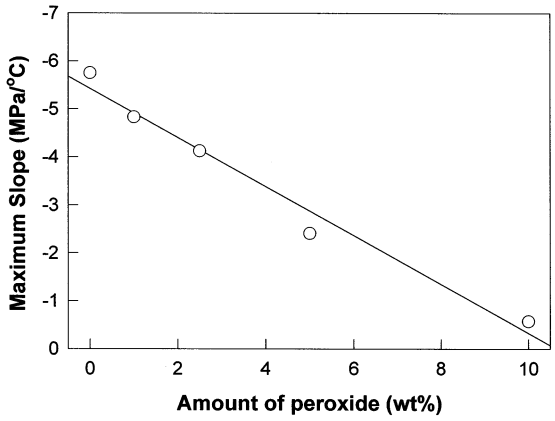

Figure 5. Maximum slopes of DMA curves for the temperature region just above the melting transition vs the weight percentage of DCP used in chemical cross-linking.

not show such outstanding shape fixing and recovery effects, a finding anticipated from DMA results that revealed poor elasticity above the melting transition. Thus, tensile stress applied to the sample above the melting transition relaxes somewhat so that it is not entirely stored upon crystallization, and the primary shape cannot be restored at elevated temperature for reasonable observation times (data not shown). Here we should mention that the density of the PCO is smaller than that of hot water; hence, during strain recovery in our configuration, the polymer must fight buoyancy. Very recently, Lendlein et al. reported shape memory properties of oligo(ϵ-caprolactone)/*n*-butyl acrylate copolymer.[6] There, it was demonstrated that shape recovery of the copolymer required 20 s to be completed at 70 °C. Compared to their results, our cured PCO sample exhibits quite rapid shape recoverability; however, testing was performed with distinct protocols so that a direct comparison is not possible.

To quantitatively evaluate the transition speed, the time evolution of curvature ($\kappa = 1/r$, r = radius of circle superposing the curved film) for the recovering samples was determined by image processing and plotted vs time as shown in Figure 7. By comparing the curvature relaxation plots for different samples, it is clear that neat PCO does not recover to the original shape of $\kappa = 0$, at least not within 5 s (data beyond the plot range shown) while cross-linked PCO samples show shape memory behavior that is faster and more complete with increasing cross-link density. Of the samples tested, 5% peroxide shows the best shape memory behavior at 70 °C. Considering the WAXS data presented in Figure 2 and Table 3, the speed of recovery (maximum slopes of plots in Figure 7) increases with decreasing degree of crystallinity, so long as the sample is cross-linked. Additionally, the extent of recovery increases with the degree of crosslinking up to 2.5% of DCP. Beyond this level of cross linking, increases in cross linking have little effect on the extent of recovery, suggesting the existence of an optimal DCP composition near 5 wt %.

On the basis of all of our characterization data reported above, including WAXS, DSC, DMA, and shape recovery experiments, we show in Figure 8 a schematic representation of the shape memory effect in chemically cross linked PCO or otherwise cross linked semicrystalline polymers. In this schematic, a cross-linked sample at room temperature (*primary shape*, (a)) is heated to melt the crystals (b), resulting in a compliant transparent material. This film can be easily stretched

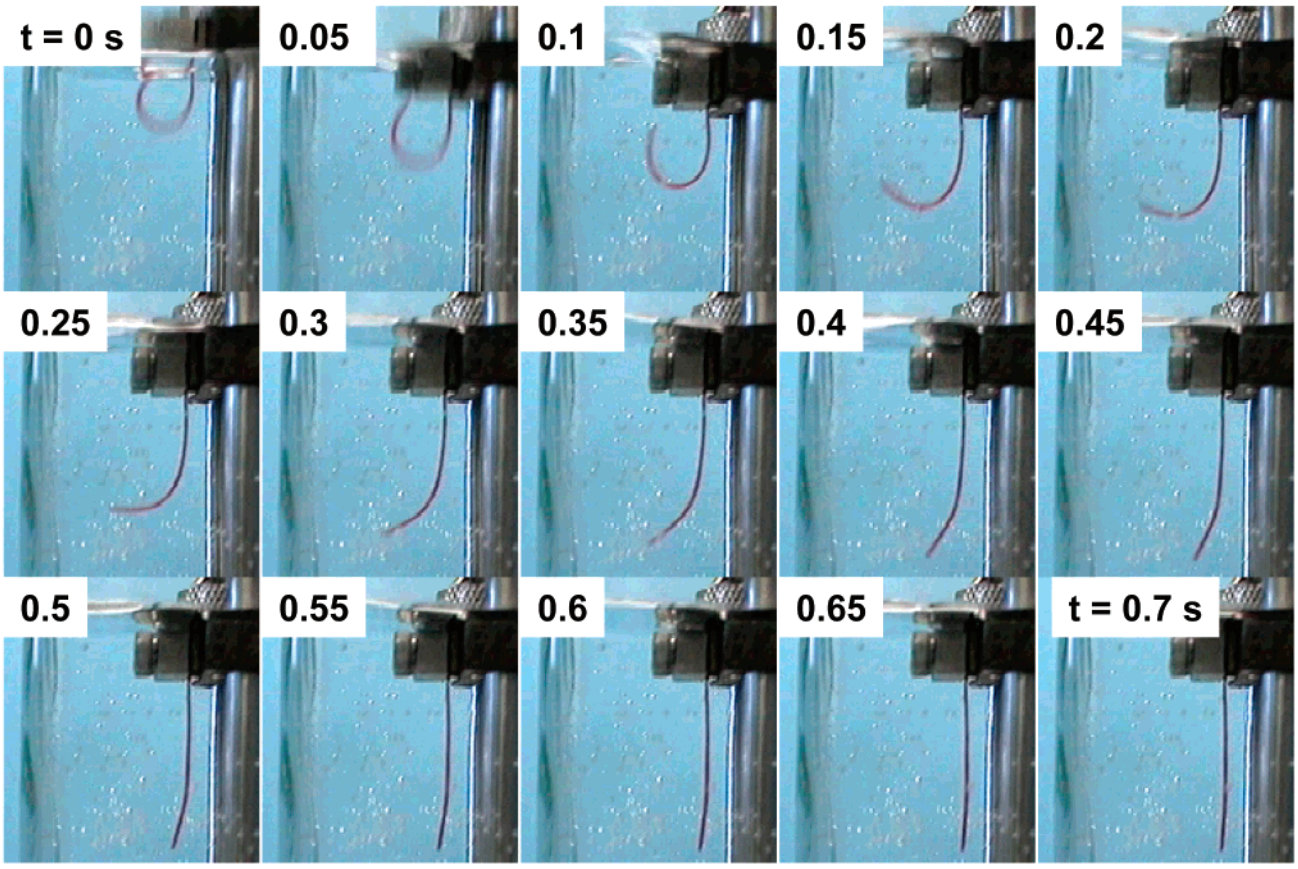

Figure 6. Shape memory behavior of PCO with DCP 2.5% following rapid immersion in water at $T = 70$ °C. The sample undergoes the transition from temporary shape (circular) to permanent (linear) within 0.7 s. The sample is colored in red.

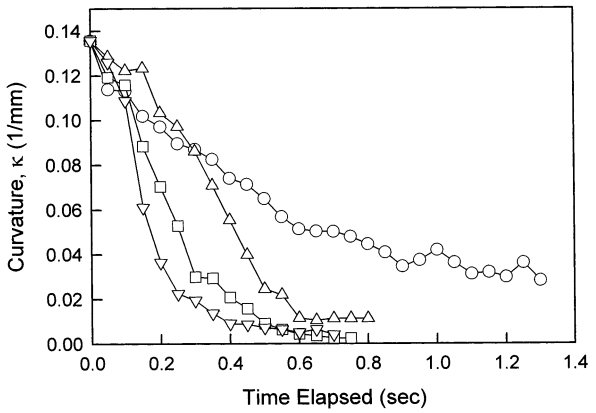

Figure 7. Curvature, κ, vs time elapsed at $T = 70$ °C: PCO5−0 (○), PCO5−1 (△), PCO5−2.5 (□), and PCO5−5 (▽).

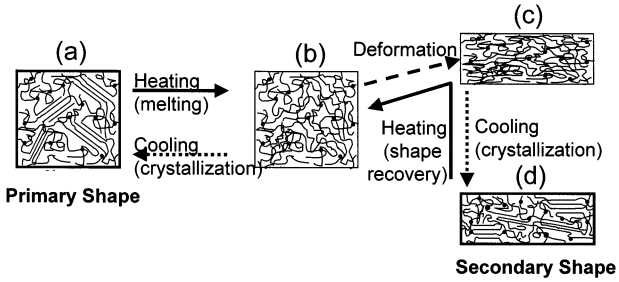

Figure 8. Schematic depiction of the microstructural transformations during a shape memory cycle of chemically cross-linked PCO. Depictions in bold frames represent temperatures below the melting point, while others are above it. Cross-linking junctions are depicted as solid black circles. See text for a complete description.

to a deformed state (c) that is fixed to a *secondary shape* (d) by cooling and crystallization. Upon heating the secondary shape, a rapid sequence of melting, (d)−(c), and then elastic recovery, (c)−(b), occurs to yield the net effect of shape memory.

Conclusions

In this study, we have prepared PCO polymers with control over the trans/cis double bond composition and molecular weight afforded by the use of ruthenium catalysts. Selected samples were cured using dicumyl peroxide of varying concentration, and the influence of cross-linking on thermal, microstructural, and thermomechanical properties was investigated. In addition, desirable shape memory characteristics were investigated for their dependence on degree of cross-linking, revealing competing influences of crystallinity for shape-fixing, seen to decrease with cross-linking, and rubber elasticity above T_m, observed to increase with cross-linking as expected. While neat, linear, PCO does not exhibit shape memory effect due to the lack of a rubbery plateau above melt transition temperature, a small amount of peroxide cross-linking (~1%) imparts shape memory effect to PCO. We observed a fast shape memory effect for the cross-linked PCO that results when crystallization-fixed distorted samples are submerged in a warm water bath. In the case of PCO containing either 2.5 or 5% peroxide, complete shape recovery from a curvature, $\kappa = 0.14$ mm^{-1}, to zero curvature occurs within 0.7 s at 70 °C.

Acknowledgment. E.B.C. thanks the NSF Materials Research Science and Engineering Center (DMR 9809365) at UMass for partial support of this work. P.T.M. acknowledges the support of Boston Scientific Corp.

References and Notes

(1) Vernon, L. B.; Vernon, H. M. (The Vernon-Benshoff Co.) US Patent 2,234,993, 1941.
(2) Kobayashi, K.; Hayashi, S. (Mitsubishi Heavy Industries, Ltd., Japan) Japan Patent 02183132, 1990.
(3) Nakayama, K. *Int. Polym. Sci. Technol.* **1991**, *18*, T/43−48.
(4) Irie, M. *Shape Memory Polymers*; Cambridge University Press: Cambridge, UK, 1998.
(5) Takechi, M.; Doi, H.; Harima, H. *Jpn. Kokai Tokkyo Koho JP 62192440 A2* **1987**, 6.
(6) Landlein, A.; Schmidt, A. M.; Langer, R. *Proc. Natl. Acad. Sci. U.S.A.* **2001**, *98*, 842−847.
(7) Boochathum, P.; Prajudtake, W. *Eur. Polym. J.* **2001**, *37*, 417−427.
(8) Boochathum, P.; Chiewnawin, S. *Eur. Polym. J.* **2001**, *37*, 429−434.
(9) Schwab, P.; Grubbs, R. H.; Ziller, J. W. *J. Am. Chem. Soc.* **1996**, *118*, 100−110.
(10) Bielawski, C. W.; Grubbs, R. H. *Angew. Chem.* **2000**, *39*, 2903−2906.
(11) Calderon, N.; Morris, M. C. *J. Polym. Sci., Polym. Phys. Ed.* **1967**, *5*, 1283−1292.
(12) Natta, G.; Bassi, I. W.; Fagherazzi, G. *Eur. Polym. J.* **1967**, *3*, 339−352.
(13) Bassi, I. W.; Fagherazzi, G. *Eur. Polym. J.* **1968**, *4*, 123−132.
(14) Schneider, W. A.; Muller, M. F. *J. Mol. Catal.* **1988**, *46*, 395−403.
(15) Yeh, G. S. Y.; Chen, C. J.; Boose, D. C. *Colloid Polym. Sci.* **1985**, *263*, 109−15.

MA021141J